

Online Multi-Task Offloading for Semantic-Aware Edge Computing Systems

Xuyang Chen, *Student Member, IEEE*, Qu Luo, *Graduate Student Member, IEEE*, Gaojie Chen, *Senior Member, IEEE*, Daquan Feng, *Member, IEEE*, and Yao Sun, *Senior Member, IEEE*

Abstract—Mobile edge computing (MEC) provides low-latency offloading solutions for computationally intensive tasks, effectively improving the computing efficiency and battery life of mobile devices. However, for data-intensive tasks or scenarios with limited uplink bandwidth, network congestion might occur due to massive simultaneous offloading nodes, increasing transmission latency and affecting task performance. In this paper, we propose a semantic-aware multi-modal task offloading framework to address the challenges posed by limited uplink bandwidth. By introducing a semantic extraction factor, we balance the relationship among transmission latency, computation energy consumption, and task performance. To measure the offloading performance of multi-modal tasks, we design a unified and fair quality of experience (QoE) metric that includes execution latency, energy consumption, and task performance. Lastly, we formulate the optimization problem as a Markov decision process (MDP) and exploit the multi-agent proximal policy optimization (MAPPO) reinforcement learning algorithm to jointly optimize the semantic extraction factor, communication resources, and computing resources to maximize overall QoE. Experimental results show that the proposed method achieves a reduction in execution latency and energy consumption of 18.1% and 12.9%, respectively compared with the semantic-unaware approach. Moreover, the proposed approach can be easily extended to models with different user preferences.

Index Terms—Mobile edge computing, resource allocation, task offloading, semantic-aware.

I. INTRODUCTION

THE sixth generation (6G) of mobile communication is demonstrating its revolutionary potential, portending the arrival of an era of ultra-massive connectivity and the Internet of Things (IoT). The volume of data generated by a vast number of devices is experiencing an explosive surge. Various compute-intensive services, such as holographic communication, extended reality (XR), and autonomous driving continue to evolve, which increasingly burden user equipments (UEs) with heavy computational demands. However, the limited computational power and battery capacity of UEs make it challenging to support a multitude of computationally intensive

Xuyang Chen is with the College of Electronics and Information Engineering, Shenzhen University, Shenzhen 518060, China, and also with the 5GIC & 6GIC, Institute for Communication Systems, University of Surrey, GU2 7XH Guildford, U.K. (email: chenxuyang2021@email.szu.edu.cn).

Daquan Feng is with the College of Electronics and Information Engineering, Shenzhen University, Shenzhen 518060, China (email: fdquan@szu.edu.cn).

Qu Luo and Gaojie Chen are with the 5GIC & 6GIC, Institute for Communication Systems, University of Surrey, GU2 7XH Guildford, U.K. (e-mail: : q.u.luo@surrey.ac.uk; gaojie.chen@surrey.ac.uk).

Yao Sun is with the James Watt School of Engineering, University of Glasgow, Glasgow, G12 8QQ, U.K. (email: Yao.Sun@glasgow.ac.uk).

tasks. Cloud computing is considered capable of alleviating the computational pressure on UEs to some extent [1]. Offloading tasks to the cloud, which has abundant computing resources, significantly reduces local computational pressure. However, the high latency associated with cloud offloading is intolerable for latency-sensitive tasks. Furthermore, the centralized model of cloud computing poses data privacy and security issues. To address the aforementioned challenges, mobile edge computing (MEC) is considered an effective solution. Edge servers (ES) near the user can provide considerable computing and storage resources, which can be fully utilized by UEs distributed. Compared to cloud computing, MEC significantly reduces latency, while its distributed computing resources ensure user privacy and security.

Nevertheless, when tasks involve substantial data transfers, such as high-definition (HD) video processing [2], virtual reality (VR) applications [3], or real-time data analytics [4], the increased volume of data transmission imposes higher demands on channel quality to meet latency requirements. In such cases, semantic communication (SemCom) can provide an effective solution. SemCom, different from the traditional bit workflow based on Shannon's information theory [5], has demonstrated great potential for enhancing the efficiency and reliability of data transmission across various task scenarios, including text [6]–[8], image [9]–[11], video [12]–[14], XR [15]–[17], and multi-modal tasks [18]–[20]. By transmitting a compact semantic representation of task data, substantial bandwidth can be saved, ensuring high quality of service (QoS).

A. Related Works

MEC technology has attracted widespread attention from academia and industry [21] due to its ability to enhance the computing capabilities of UEs and improve the quality of service (QoS). In [22], the authors optimized the allocation of communication, computation, and energy resources based on a perturbed Lyapunov algorithm, maximizing system throughput under the stability constraints of task and energy queues. A power minimization method with task buffer stability constraints was proposed in [23], where the Lyapunov optimization algorithm was used to solve computing offloading strategies. Liu et al. considered the requirements for ultra-reliable and ultra-low latency (URLLC) tasks [24], applying extreme value theory to minimize user power consumption while satisfying probabilistic queue length constraints.

However, the aforementioned model-based approaches are typically computationally intensive, further burdening user de-

vices. Moreover, model-based methods often require multiple iterations to find the optimal offloading strategy, which is intolerable for latency-sensitive tasks and impractical in rapidly changing wireless channel conditions. To address these issues, resource allocation and computation offloading methods based on Deep Reinforcement Learning (DRL) were proposed. The authors of [25] modeled the computation offloading as a multi-stage stochastic mixed-integer nonlinear programming (MINLP) problem and solved it using a combination of Lyapunov optimization and a DRL model, integrating the advantages of both model-based and DRL approaches. In [26], [27], the authors exclusively utilized DRL to solve for joint strategies of computation offloading and resource allocation, similarly achieving quite impressive results.

For services like holographic communication [28] and real-time video analysis [29], which are both latency-sensitive and compute-intensive, ensuring consistent QoS is challenging due to the need to transmit large amounts of data while combating wireless channel fading. Elaborate deep neural networks are often used for such sophisticated tasks, however, they also introduce significant computational and storage burdens on devices, necessitating the leverage of ES computing power through integration with MEC. Although offloading tasks to the ES can alleviate the computational burden on UEs and reduce execution latency, excessive data offloading or too many UEs offloading simultaneously can lead to network congestion, resulting in offloading failures.

Given these considerations, it is essential to design a semantic-aware MEC system by combining MEC with SemCom [30]. By performing semantic extraction on the data to be offloaded, UEs can filter out data irrelevant to the task, thereby reducing network traffic. In [31], the authors defined a semantic entropy to quantify the semantic information of different tasks. Deep Q-Network (DQN) and many-to-one matching algorithms are used to solve the joint optimization problem of semantic compression, channel allocation, and power distribution in multi-cell multi-task scenarios. A semantic-aware resource allocation method was proposed in [32], introducing a semantic-aware factor to characterize the relationship between semantic compression rate and computational overhead, aiming to balance the degree of semantic compression. The authors of [33] proposed a semantic-aware cloud-edge-end collaborative networking method to utilize distributed computing resources and also proposed a multi-modal task offloading system in [34], where a unified QoE metric was designed.

B. Motivations and Contributions

In traditional MEC scenarios, computational and communication resources are often jointly optimized to minimize system energy consumption [35] or execution latency [36], or a combination of both [37]. However, these approaches lack consideration for task execution performance and comprehensive QoE. 6G strives to provide stable, reliable, and high-quality personalized services to each user [38]. Preferences often vary among different users and types of services. For instance, in MEC scenarios, users dealing with latency-sensitive tasks may

prefer lower latency, those pursuing task performance may favor better task execution accuracy, while users with limited battery power might opt for task offloading strategies that consume less power. Therefore, a good QoE metric should encompass the preferences of different users. Additionally, since each user may need to handle multi-modal tasks, the complexity and evaluation metrics of different tasks vary. For example, bimodal tasks like visual question answering (VQA) typically require more processing time and computational resources compared to text translation, and their evaluation metrics are entirely different.

Semantic-aware MEC systems have been studied in [31]–[34]. Nonetheless, In [31]–[33], the authors did not address multi-modal tasks or design a unified QoE metric. The authors of [34] did not consider the impact of semantic extraction on task execution latency and performance. To address the aforementioned challenges, we investigate resource allocation schemes in multi-modal task offloading that coordinate computational and communication resources through semantic compression-aware methods. To fairly compare the offloading performance of different task modalities, a unified QoE metric is proposed. Computational and communication resources are jointly optimized to maximize the overall QoE for UEs. The main contributions of this paper are summarized as follows:

- We propose a novel semantic-aware task offloading system for multi-modal tasks. The SemCom systems for image classification, text classification, and VQA are first constructed to compress source data into compact semantic representations. The semantic extraction factor is used to characterize the degree of data compression, which affects the task's execution latency, energy consumption, and performance.
- We design a unified and fair QoE evaluation metric that addresses the challenges posed by the diverse distribution of user task types and the lack of uniform task evaluation criteria. Specifically, the QoE metric comprises three components: task execution latency, task execution energy consumption, and task execution performance. We employ a unified logistic function to normalize these three components, thereby obtaining a unified and comparable QoE.
- The joint optimization for semantic extraction factor, computational resources, and communication resources is performed using the MAPPO algorithm, maximizing the overall QoE. Users solve for the optimal channel allocation, power allocation, semantic extraction level, and computation offloading scheme according to their observed task sizes and channel conditions.
- Comprehensive experiments demonstrate the effectiveness of the proposed approach. Compared to the semantic-unaware method, the proposed algorithm achieves a reduction in execution latency and energy consumption of 18.1% and 12.9%, respectively. Additionally, the proposed approach can meet user preferences for various metrics such as execution latency, energy consumption, and execution performance.

The remainder of this paper is organized as follows. Section

II describes the semantic-aware transmission and computation model, defines the unified QoE metric, and formulates the problem as maximizing overall QoE. Section III introduces solving the QoE maximization problem using the MAPPO algorithm, providing training details. Section IV presents relevant experimental details and simulation results. Finally, Section V outlines our conclusions.

II. SYSTEM MODEL AND PROBLEM FORMULATION

We propose a novel semantic-aware multi-modal task offloading system, as shown in Fig. 1, where UEs employ an orthogonal frequency-division multiple access (OFDMA) scheme. At the access point (AP), K resource blocks are allocated to serve N users at different sub-channels. The set of UEs and sub-channels are defined as $\mathcal{N} = \{1, 2, \dots, N\}$ and $\mathcal{K} = \{1, 2, \dots, K\}$. The length of the UE _{n} 's task queue is denoted as Q_n . The task currently being executed by the UE _{n} is represented by q_n^M , where $M \in \{\mathcal{T} : \text{text}, \mathcal{I} : \text{image}, \mathcal{B} : \text{VQA}\}$. Hence, each UE is associated with three potential task types: text classification, image classification, and VQA. We assume that tasks are atomic [34], i.e. all tasks are either executed locally or offloaded to the ES. The illustrations of the main notations are summarized in Table I.

A. Semantic-Aware Model

Traditional MEC offloading methods usually require transmitting all data to the ES. SemCom enables the extraction of task-relevant semantic information, reducing bandwidth consumption while enhancing robustness to channel variations. Based on this, we propose a semantic-aware multi-modal task offloading framework. Fig. 2 illustrates the process of semantic-aware offloading. While semantic extraction indeed reduces the volume of data transmitted, the associated increase in semantic extraction latency and computational burden must also be comprehensively considered. Hence, we define a semantic extraction factor $\mu_n \in [\mu_n^{\min}, 1]$. The semantic extraction module determines the level of data compression. When $\mu_n = 1$, the UE transmits all data instead of semantic information. Transmitting all data can achieve better task performance but imposes a heavy transmission burden. The smaller the μ_n , the greater the level of semantic compression, which significantly reduces the transmission load. However, semantic extraction introduces additional computational overhead and may decrease task performance on the ES. The minimum value μ_n^{\min} is typically determined by task accuracy requirements and user battery capacity. Therefore, selecting μ_n requires a comprehensive evaluation of the current task computational load, channel environment, user battery capacity, and other relevant information.

B. Transmission Model

The channel gain from UE _{n} to ES via sub-channel k is denoted by $|g_{k,n}|^2 = |h_{k,n}|^2/d_n^{-\alpha}$, where $h_n \sim \mathcal{CN}(0, 1)$ is Rayleigh fading coefficient, and d_n is the distance from UE _{n} to ES, and α is the path loss exponent, and $\mathcal{CN}(0, 1)$ is the

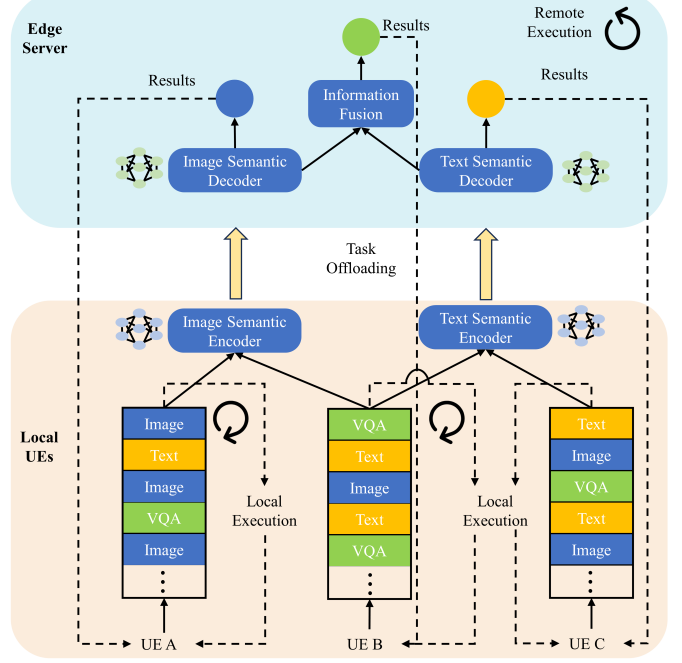


Fig. 1. Semantic-aware multi-task offloading system model.

complexed Gaussian distribution with zero mean and variance one. The transfer function can be represented as

$$y_n = g_{k,n}\sqrt{p_n}s_n + n_z, \quad (1)$$

where p_n denotes the transmit power from UE _{n} to ES, and s_n is the normalized transmission data from UE _{n} to ES, and $n_z \sim \mathcal{CN}(0, \sigma_z^2)$ is zero-mean additive white Gaussian noise (AWGN) with noise power σ_z^2 . The maximum achievable offloading data rate from UE _{n} to ES can be represented as

$$R_{k,n} = B \log_2 \left(1 + \frac{g_{k,n}p_n}{\sigma_z^2} \right), \quad (2)$$

where B is the channel bandwidth. Therefore, the transmission latency can be expressed as

$$t_n = \frac{\rho_n s_n \mu_n^p}{R_{k,n}}, \quad (3)$$

where $p > 0$ is a constant parameter. ρ_n is a binary variable, where $\rho_n = 1$ represents offloading tasks to ES, and $\rho_n = 0$ denotes local computation. In comparison to the amount of data required for task offloading, the computation results typically involve a much smaller data size [39], [40], therefore, we only consider the upload rate and latency.

C. Computation Model

The computation latency of UE _{n} can be denoted as

$$t_n^U = \begin{cases} \frac{(1-\rho_n)l_n^U}{c_n}, & \text{if } \mu_n = 1, \\ \frac{(1-\rho_n)l_n^U}{c_n} + \frac{\rho_n l_n^{SE}}{\mu_n^k c_n}, & \text{otherwise,} \end{cases} \quad (4)$$

where l_n^U is the Graphic Processing Unit (GPU) consumption of the current task computed by UE _{n} , and l_n^{SE} is the basic GPU consumption of semantic extraction. l_n^U and l_n^{SE} are

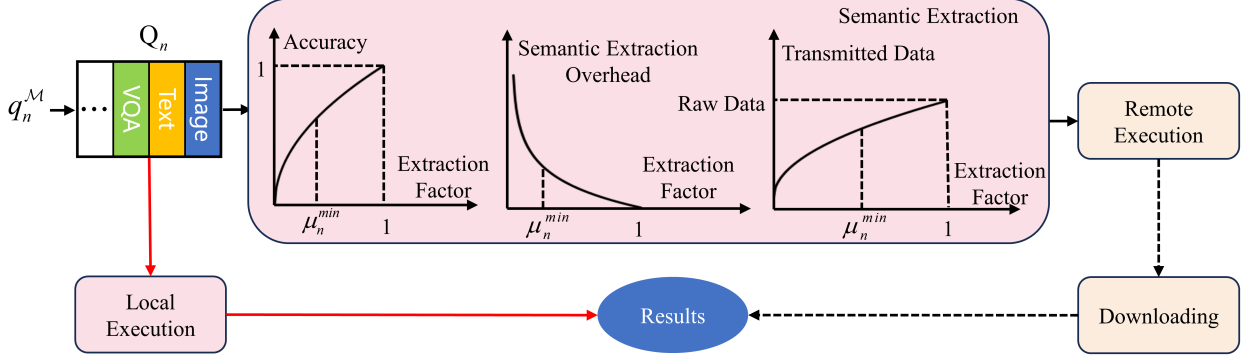


Fig. 2. Semantic extraction workflow. The semantic extraction factor alters the degree of semantic compression, affecting the computational burden of semantic extraction, the volume of data transmission, and the accuracy of task execution.

TABLE I
NOTATIONS AND SYMBOLS

Notation	Explanation
\mathcal{N}	The set of all UEs
\mathcal{K}	The set of all sub-channels
\mathcal{M}	The set of task modalities
μ_n	The semantic extraction factor
$g_{k,n}$	The channel gain from UE $_n$ to ES via sub-channel k
$R_{k,n}$	The maximum offloading rate from UE $_n$ to ES via sub-channel k
B	The channel bandwidth
ρ_n	The offloading decision
s_n	The transmitted message
t_n	The transmission latency
t_n^U	The computation time of UE $_n$
l_n^U	The GPU consumption executed by UE $_n$
l_n^{SE}	The basic GPU consumption of semantic extraction
c_n	The GPU computation capability of UE $_n$
t_n^S	The computation time of ES
l_n^S	The GPU consumption executed by ES
c_s	The GPU computation capability of ES
t_n^M	The execution time of task q_n^M
E_n^U	The energy consumption of UE $_n$
κ^U	The energy coefficient of UE $_n$
f_n	The GPU clock frequency of UE $_n$
E_n^S	The energy consumption of ES
κ^S	The energy coefficient of ES
f_s	The GPU clock frequency of ES
ε_n^M	The accuracy of task M
QoE_n	The QoE of UE $_n$
G_M^t, G_M^e, G_M^a	The functions of execution time, energy consumption, and task accuracy score, respectively
$\omega_t, \omega_e, \omega_a$	The weights of execution time, energy consumption, and task accuracy, respectively

related to the corresponding task M . $k > 0$ is a constant parameter. $c_n = o_n f_n$ is the GPU computation capability of UE $_n$. o_n represents the floating-point operations (FLOPS) executed per cycle by the GPU of UE $_n$ and f_n denotes the GPU clock frequency of UE $_n$. When tasks are offloaded to ES, the computation time of tasks on the ES can be expressed as

$$t_n^S = \frac{l_n^S c_s}{\sum_{n \in \mathcal{N}} \rho_n}, \quad (5)$$

where l_n^S is the GPU consumption of the current task computed by ES. $c_s = o_s f_s$ denotes the GPU computation capability of ES. o_s represents the FLOPS executed per cycle by the GPU of ES and f_s denotes the GPU clock frequency of ES. The computational resources of the ES are evenly distributed among all users currently being served. Combining the aforementioned factors, the processing latency of UE $_n$'s current task q_n^M can be expressed as

$$\begin{aligned} t_n^M &= \rho_n (t_n + t_n^U + t_n^S) + (1 - \rho_n) t_n^U \\ &= \rho_n (t_n + t_n^S) + t_n^U. \end{aligned} \quad (6)$$

D. Energy Consumption Model

The energy consumption of UE $_n$ can be written as

$$E_n^U = \kappa^U t_n^U f_n^3 + p_n t_n, \quad (7)$$

where κ^U is the energy coefficient of UE $_n$. The energy consumption of ES can be described as [34]

$$E_n^S = \kappa^S t_n^S \left(\frac{f_s}{\sum_{i \in \mathcal{I}} \rho_n} \right)^3, \quad (8)$$

where κ^S is the energy coefficient of ES. Therefore, the energy consumption of UE $_n$'s current task q_n^M can be expressed as

$$E_n^M = E_n^U + E_n^S. \quad (9)$$

E. Multi-Task Offloading Design and Problem Formulation

We consider three types of tasks: image classification, text classification, and VQA, all of which can be evaluated using accuracy to measure task performance:

$$\varepsilon_n^M = f^M(s_n, \nu_n), \quad (10)$$

where ε_n^M is the accuracy of task M , and $f^M(\cdot)$ is the pretrained semantic transmission model for modality M , and ν_n is SNR. Once the model training is completed, we can directly calculate the number of FLOPS required by the UE's semantic encoder to determine the basic GPU consumption l_n^{SE} for semantic extraction. Similarly, we compute the number of FLOPS required by the ES's semantic decoder to determine the GPU consumption l_n^S for the ES. To evaluate the performance of offloading tasks for different UEs, it is essential to define a unified QoE standard.

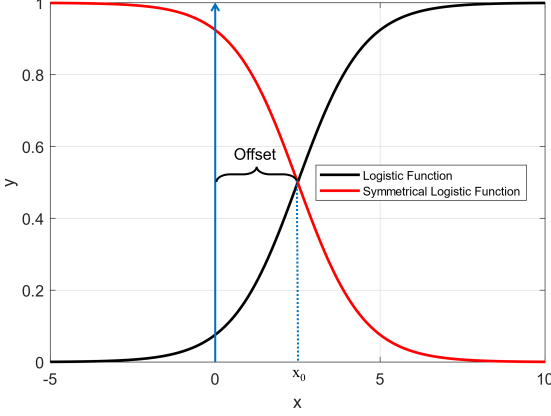


Fig. 3. QoE function. The logistic function serves as the scoring function for task accuracy, with its symmetric function scoring execution latency and energy consumption. The offset x_0 represents the latency, energy consumption, or task accuracy of local execution.

The performance of task execution is associated with computation time, energy consumption, and task accuracy. However, defining a fair and reasonable QoE is challenging. When tasks of different modalities are unevenly distributed among different UEs, directly calculating the weighted sum of energy consumption, computation time, and task accuracy is unfair. Typically, text tasks have lower computation time and energy consumption than image tasks, while image tasks have lower computation time and energy consumption than VQA tasks. Additionally, the accuracies of different tasks are usually incomparable. Inspired by [41]–[43], we propose a QoE calculation method that can fairly compare task execution performance across different UEs:

$$\begin{aligned} \text{QoE}_n &= \sum_{q_n^{\mathcal{M}}=1}^{Q_n} (\omega_t G_{\mathcal{M}}^t + \omega_e G_{\mathcal{M}}^e + \omega_a G_{\mathcal{M}}^a) \\ &= \sum_{q_n^{\mathcal{M}}=1}^{Q_n} \left(\frac{\omega_t}{1 + e^{-\lambda(t_n^l - t_n^{\mathcal{M}})}} + \frac{\omega_e}{1 + e^{-\beta(E_n^l - E_n^{\mathcal{M}})}} \right. \\ &\quad \left. + \frac{\omega_a}{1 + e^{-\eta(\varepsilon_n^{\mathcal{M}} - \varepsilon_n^l)}} \right), \end{aligned} \quad (11)$$

where ω_t , ω_e and ω_a are the weights of computation time, energy consumption, and task accuracy, respectively. The sum of ω_t , ω_e and ω_a are equal to 1. $t_n^l = l_n^U/c_n$ denotes the task execute delay by UE_n. As shown in Fig. 3, we use the logistic/sigmoid function and its symmetrical counterpart for QoE calculations. Corresponding latency score $G_{\mathcal{M}}^t$ and energy consumption score $G_{\mathcal{M}}^e$ are calculated using the symmetric logistic function, while accuracy score $G_{\mathcal{M}}^a$ is measured with the logistic function. The offset x_0 represents local execution latency, energy consumption, or accuracy. Specifically, $E_n^l = \kappa^U t_n^U (f_n)^3$ denotes the task execution energy consumption by UE_n. ε_n^l denotes the task executes accuracy by UE_n. That is, we normalize the QoE using the latency, energy consumption, and accuracy of tasks executed locally by the UE.

Mathematically, the optimization problem can be formulated

as

$$(\mathbf{P0}) \quad \underset{\{\rho, p, f, x, \mu\}}{\text{maximize}} \quad \sum_{i=1}^I \sum_{q_n^{\mathcal{M}}=1}^{Q_n} x_{k,n} \text{QoE}_i \quad (12a)$$

$$\text{s.t. } \rho_n \in \{0, 1\}, \quad \forall n \in \mathcal{N}, \quad (12b)$$

$$x_{k,n} \in \{0, 1\}, \quad \forall n \in \mathcal{N}, \forall k \in \mathcal{K}, \quad (12c)$$

$$\sum_{k=1}^{\mathcal{K}} x_{k,n} = 1, \quad \forall n \in \mathcal{N}, \quad (12d)$$

$$\sum_{n=1}^{\mathcal{N}} x_{k,n} = 1, \quad \forall k \in \mathcal{K}, \quad (12e)$$

$$\mu_n^{\min} \leq \mu_n \leq 1, \quad \forall n \in \mathcal{N}, \quad (12f)$$

$$p_n \leq p_{\max}, \quad \forall n \in \mathcal{N}, \quad (12g)$$

$$f_n \leq f_{\max}, \quad \forall n \in \mathcal{N}, \quad (12h)$$

$$t_n^{\mathcal{M}} \leq t_{\max}, \quad \forall n \in \mathcal{N}, \quad (12i)$$

$$E_n^{\mathcal{M}} \leq E_n^{\max}, \quad \forall n \in \mathcal{N}, \quad (12j)$$

$$\varepsilon_n^{\mathcal{M}} \geq \varepsilon_{\min}, \quad \forall n \in \mathcal{N}, \quad (12k)$$

$$n = 1, 2, \dots, N, \quad (12l)$$

where $\{\rho, p, f, x, \mu\} = \{\rho_n, p_n, f_n, x_{k,n}, \mu_n\}, \forall n \in \mathcal{N}, \forall k \in \mathcal{K}$. $x \in \mathbb{R}^{K \times N}$ denote the collection of all sub-channel allocation indicators $x_{k,n}$. $x_{k,n} = 1$ indicates UE_n is assigned to sub-channel k , $x_{k,n} = 0$ otherwise. In (P0), (12b) and (12c) represent the offloading choice and channel selection constraints, respectively. Constraint (12d) and (12e) indicate that each UE is assigned to one sub-channel and each sub-channel is occupied by one UE. p_{\max} in (12g) is the maximum transmit power constraint, f_{\max} in (12h) is the maximum GPU frequency of UE_n, t_{\max} in (12i) is the maximum execute latency constraint, E_n^{\max} in (12j) is the battery capacity of UE_n, and ε_{\min} in (12k) is the minimum task accuracy requirement, which is dependent on the modality \mathcal{M} of the current task.

III. MULTI-AGENT PROXIMAL POLICY OPTIMIZATION FOR RESOURCE ALLOCATION

The binary offloading variable in Constraint (12b) introduces non-convexity, and the QoE is characterized by a non-convex logistic function, rendering the problem **P0** a non-convex MINLP problem. To solve the non-convex MINLP problem **P0**, we employ an advanced MAPPO algorithm, an actor-critic-based reinforcement learning algorithm, which is suitable for both discrete and continuous action spaces. To utilize the MAPPO algorithm, we reformulate problem **P0** as an MDP problem and detail the training process of the MAPPO.

A. Problem Reformulation Based on MDP

A 4-tuples MDP $\langle \mathcal{S}, \mathcal{A}, \mathcal{R}, \gamma \rangle$ is used to describe the interaction between the ES and the wireless network. where \mathcal{S} , \mathcal{A} , \mathcal{R} and $\gamma \in [0, 1]$ denote the state space, action space, reward function, and the discount factor, respectively. As agents, UEs need to collect observable states to input into the policy

network and obtain their actions. After executing actions, UEs update their observable states and the policy network based on corresponding rewards to improve the output of actions. Specifically, the observable state of UE_n can be represented as $o_n = \{g_{k,n}, l_n^U, l_n^S\} \in \mathcal{S}$. The action space of UE_n refers to the variables that need to be optimized, which can be expressed as $a_n = \{\rho_n, p_n, f_n, \mu_n, x_{k,n}\} \in \mathcal{A}$. UEs need to continuously optimize offloading strategies, transmit power, local computation frequency, semantic compression ratio, and channel assignment to purchase better QoE. Drawing from the optimization problem **P0**, it is evident that the reward function needs to focus on the summation QoE of all UEs. In addition to QoE, the reward function includes penalty terms for latency and task accuracy, expressed as

$$r_n = \begin{cases} QoE_n & \text{successful task execution,} \\ t_{max} - t_n & \text{if (12i) not satisfied,} \\ E_n^{max} - E_n^M & \text{if (12j) not satisfied,} \\ \varepsilon_n^M - \varepsilon_{min} & \text{if (12k) not satisfied.} \end{cases} \quad (13)$$

Therefore, the total reward at the t th training timestep is defined as $r_t = \sum_{n=1}^N r_n$. The cumulative long-term reward to account for the impact of the current state and action on the expected future rewards:

$$R_t(\tau) = \sum_{t'=t}^T \gamma^{t'-t} r_{t'}, \quad (14)$$

where τ is a completed trajectory. Let π_θ represents a policy parameterized by θ , where a_t is the collection of a_n at time t , and s_t is the collection of o_n at time t . Given the state s_t , the probability of taking action a_t under policy π_θ is denoted as $\Pr(a_t | s_t, \pi_\theta)$. Consequently, the expected discounted rewards under policy π_θ , denoted as $J(\pi_\theta)$, can be expressed as

$$J(\pi_\theta) = \mathbb{E}_{a_t \sim \pi_\theta, s_t \sim \mathcal{P}} \left[\sum_{t=1}^T \gamma^{t-1} r_t(s_t, a_t) \right]. \quad (15)$$

UEs seek to find the optimal policy π_θ to maximize the expected cumulative reward $J(\pi_\theta)$. Therefore, the optimization problem **P0** is reformulated as an MDP problem:

$$\begin{aligned} & \max_{\pi_\theta} J(\pi_\theta) \\ & \text{s.t. } a_t \sim \pi_\theta(a_t | s_t), s_{t+1} \sim \Pr(s_{t+1} | s_t, a_t). \end{aligned} \quad (16)$$

B. PPO-Based Algorithm

For on-policy gradient algorithms, trajectories are typically sampled using a fixed policy π_θ , and policy updates are made using only those trajectories sampled by π_θ . Fig. 4 illustrates our proposed PPO-based algorithm. PPO is an off-policy algorithm that improves sampling efficiency significantly. It utilizes an experience replay buffer, which stores trajectories from past time steps. Policy π_θ randomly selects trajectories from the replay buffer for updates, enhancing sampling efficiency. This implementation benefits from the use of importance sampling, as outlined in *Lemma 1*.

Lemma 1. Given distributions $x \sim p(x)$ and $x \sim q(x)$, the $\mathbb{E}_{x \sim p} f(x) = \mathbb{E}_{x \sim q} \frac{p(x)}{q(x)} f(x)$.

Proof. Given $x \sim p(x)$, the expectation of $f(x)$ can be expressed as

$$\begin{aligned} \mathbb{E}_{x \sim p} f(x) &= \int_x p(x) f(x) dx \\ &= \int_x \frac{p(x)}{q(x)} q(x) f(x) dx = \mathbb{E}_{x \sim q} \frac{p(x)}{q(x)} f(x). \end{aligned} \quad (17)$$

Using importance sampling, the optimization function for PPO can be reformulated as

$$J^{\theta'}(\theta) = \mathbb{E}_{(s_t, a_t) \sim \pi_{\theta'}} \left[\frac{p_\theta(a_t | s_t)}{p_{\theta'}(a_t | s_t)} A_t^{\theta'}(s_t, a_t) \right], \quad (18)$$

where θ is the parameter that needs to be optimized while θ' is the parameter used for sampling. $p_\theta(a_t | s_t)$ and $p_{\theta'}(a_t | s_t)$ represent taking action a_t given state s_t with θ and θ' , respectively. θ' interacts with the environment to generate trajectories while θ does not interact with the environment directly but learns from the trajectories sampled by θ' . The advantage function $A_t^{\theta'}(s_t, a_t)$ represents the advantage of state-action pairs (s_t, a_t) obtained through the interaction of θ' with the environment, which is defined as

$$A_t^{\theta'}(s_t, a_t) = Q_t^{\theta'}(s_t, a_t) - V_t^{\theta'}(s_t). \quad (19)$$

The state-action value function $Q_t^{\theta'}(s_t, a_t)$ is represented as

$$Q_t^{\theta'}(s_t, a_t) = \mathbb{E}_{a_t \sim \pi_\theta, s_t \sim \mathcal{P}} \left[\sum_{t=1}^T \gamma^{t-1} r_t \right], \quad (20)$$

and the state-value function is defined as

$$V_t^{\theta'}(s_t) = \mathbb{E}_{s_t \sim \mathcal{P}} \left[\sum_{t=1}^T \gamma^{t-1} r_t \right]. \quad (21)$$

It is noted that $Q_t^{\theta'}(s_t, a_t)$ can also be expressed by temporal difference (TD) form as $Q_t^{\theta'}(s_t, a_t) = r_t + \gamma V_t^{\theta'}(s_{t+1})$. Therefore, (19) can be reformulated as

$$A_t^{\theta'}(s_t, a_t) = r_t + \gamma V_t^{\theta'}(s_{t+1}) - V_t^{\theta'}(s_t). \quad (22)$$

However, estimating based on TD often carries a higher bias. Thus, we employ Generalized Advantage Estimation (GAE) [44] to evaluate the current state-action value function. The GAE advantage function can be expressed as

$$A_t^{GAE}(s_t, a_t) = \sum_{l=0}^{T-t} (\lambda \gamma)^l \delta_{t+l}, \quad (23)$$

where $\delta_t = A_t^{\theta'}(s_t, a_t)$. Note that (23) aims to balance the variance and bias of the advantage estimates by leveraging information from multiple future steps while discounting their influence.

If there are no constraints on the policies π_θ and $\pi_{\theta'}$, significant fluctuations may occur during policy updates. This is due to the limited sampling which fails to accurately represent the probability distributions described in *Lemma 1*. To constrain the divergence between policies π_θ and $\pi_{\theta'}$, $J^{CLIP}(\theta)$ is employed. It is defined as

$$\begin{aligned} J^{CLIP}(\theta) &= L_t^{CLIP} \\ &= \mathbb{E}_t \left[\min(r_t(\theta) A_t^{\theta'}(s_t, a_t), g(\epsilon, A_t^{\theta'}(s_t, a_t))) \right], \end{aligned} \quad (24)$$

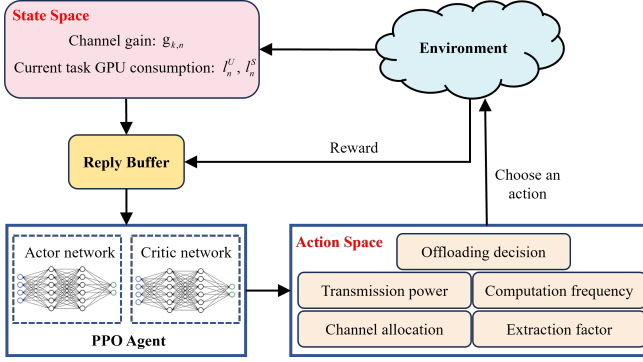


Fig. 4. The framework of PPO-based algorithm.

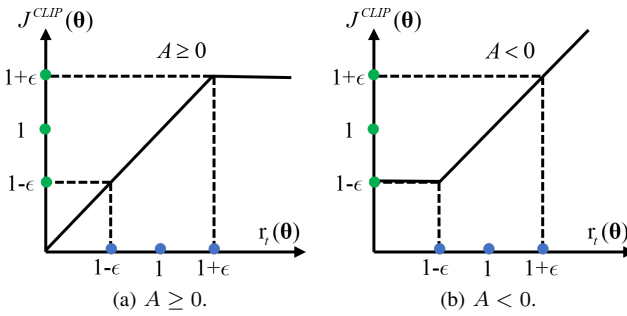


Fig. 5. The impact of A on J^{CLIP} .

where $r_t(\theta) = \frac{p_\theta(a_t|s_t)}{p_{\theta'}(a_t|s_t)}$ and g is the clip function which can be defined as

$$g(\epsilon, A_t^{\theta'}(s_t, a_t)) = \begin{cases} (1 + \epsilon) A_t^{\theta'}(s_t, a_t), & \text{if } A_t^{\theta'}(s_t, a_t) \geq 0, \\ (1 - \epsilon) A_t^{\theta'}(s_t, a_t), & \text{if } A_t^{\theta'}(s_t, a_t) < 0, \end{cases} \quad (25)$$

where ϵ is a hyperparameter, which can control the step size of the policy network updates.

Fig. 5 illustrates the impact of A on the J^{CLIP} function. Fig. (5a) and Fig. (5b) correspond to cases where $A \geq 0$ and $A < 0$, respectively. When $A \geq 0$, the state-action pair is favorable, and we aim to increase its probability; that is, the larger p_θ is, the better. However, the maximum value of $r_t(\theta)$ cannot exceed $1 + \epsilon$, meaning the ratio of p_θ to $p_{\theta'}$ should not exceed $1 + \epsilon$. When $A < 0$, the state-action pair is unfavorable, and we aim to reduce p_θ , but the ratio of p_θ to $p_{\theta'}$ should not fall below $1 - \epsilon$. By using the CLIP function, the difference between p_θ and $p_{\theta'}$ is moderate, which helps improve the model's convergence speed and performance. The loss function of the critic network aims to minimize the discrepancy between the state-value function and the cumulative reward and is expressed as

$$L_t^{\text{CL}} = \|V_t^{\theta'}(s_t) - R_t(\tau)\|^2. \quad (26)$$

To enhance the stochasticity of the policy, the final loss function for the MAPPO algorithm is formulated as

$$L_t^{\text{CL+CLIP+S}}(\theta) = \mathbb{E}_t [L_t^{\text{CLIP}} - b_1 L_t^{\text{CL}} + b_2 H(\pi_\theta(\cdot | s_t))], \quad (27)$$

Algorithm 1 MAPPO Training Algorithm

Initialization: Initialize the policy network with parameters θ , the demonstration policy network with parameters θ' and the critic network with parameters ϕ . Initialize the observation space o_n and the action space a_n .

Input: Corresponding channel gain $g_{k,n}$ and task queue Q_n .

Output: Trained neural network.

```

1: for episodes do
2:    $\pi_{\theta'} \leftarrow \pi_\theta$ ;
3:   Run policy  $\pi_{\theta'}$  for  $T$  steps and save the trajectory  $\tau$  to the replay
   buffer;
4:   Calculate  $T$  step GAE  $A_1^{\text{GAE}}, \dots, A_T^{\text{GAE}}$  using  $\pi_{\theta'}$  and  $\phi$ ;
5:   for epochs do
6:     Update  $\theta$  using (28);
7:     Update  $\phi$  using (29);
8:   end for
9: end for

```

where b_1 and b_2 are weight coefficients. H is the entropy bonus to ensure sufficient exploration.

Actor-critic based PPO algorithm comprises a policy network θ for outputting actions and a critic network ϕ . The parameters θ are updated by

$$\arg \max_{\theta} \hat{\mathbb{E}}_t [L_t^{\text{CLIP}} + b_2 H(\pi_\theta(\cdot | s_t))], \quad (28)$$

and parameters ϕ are updated by

$$\arg \min_{\phi} \hat{\mathbb{E}}_t [L_t^{\text{CL}}]. \quad (29)$$

The expectation $\hat{\mathbb{E}}_t$ is estimated using data obtained from interactions between the agent and the environment. Monte Carlo sampling is utilized to approximate the expectation $\hat{\mathbb{E}}$.

IV. SIMULATION RESULTS

In this section, the performance of the semantic-aware multi-modal task offloading model will be demonstrated. We provide specific implementation details, investigate the QoE performance of the proposed approach, and examine the impact of user preferences on the system.

A. Implementation Details

Three tasks are considered: text classification, image classification, and VQA. For text classification, we use the SST-2 dataset, for image classification, the CIFAR-10 dataset, and for VQA, the VQA2 dataset is adopted. The text semantic extraction network utilizes an advanced BERT-based [45] text embedding model, while the image semantic extraction network is based on the Vision Transformer (ViT) [46]. Training is conducted using the AdamW optimizer, with a learning rate of 3×10^{-5} , a batch size of 50, and a weight decay of 1×10^{-4} . All experiments were conducted on a platform equipped with GPU NVIDIA Titan V and CPU Intel i9-9900K @3.6 GHz. When the training of the multi-modal semantic transmission model is complete, we can calculate the GPU consumption for basic semantic extraction l_n^{SE} and the GPU consumption l^S for execution at the ES. Typically, the computational demand of the model deployed at the ES is greater than that of the local model, which leads to better task performance. Therefore, we set l_n^U (local execution GPU consumption) to be less than l^S (ES execution GPU consumption), with the task accuracy of local execution being lower than that of execution at the ES.

TABLE II
SIMULATION PARAMETERS

Parameter	Value
Number of UEs N	2
Carrier frequency	2 GHz
Sub-channel bandwidth B	2 MHz
Channel gain $g_{k,n}$ range	(0.1, 1)
Noise power σ_z^2	2 mW
Transmit power p_n range	(10, 100) mW
Semantic extraction factor μ_n	(0.3, 1)
FLOPS per cycle of local GPU o_n	2
Local GPU frequency f_n range	(0.55, 1.0) GHz
FLOPS per cycle of remote GPU o_s	4
Remote GPU frequency f_s	3 GHz
Energy consumption coefficient of UEs α^U	1×10^{-26}
Energy consumption of ES α^S	5×10^{-27}
Minimum accuracy requirements ϵ_{\min}	0.56
Execution latency constraint t_{\max}	5 ms
Training episode of the MAPPO algorithm	250
Testing episode of the MAPPO algorithm	100
Batch size of training the MAPPO	1
Epoch of training the MAPPO	5
Learning rate	5×10^{-4}
Advantage discount factor λ	0.98
Reward discount factor γ	0.95
PPO-Clip parameter ϵ	0.2
Policy entropy bonus weight b_2	0.01

We consider scenarios with two users and two orthogonal subcarriers, where each user has a queue length of 10, containing tasks from different modalities. Additional details regarding the wireless environment, GPU computational frequency, and MAPPO training configurations are summarized in Table II. To verify the effectiveness of the semantic-aware multimodal task offloading framework, we consider the following benchmarks:

- **Exhaustive search:** This method explores the entire action space to find the upper bound of the optimization problem **P0**. The action space is discretized to facilitate finding the optimal discrete solution.
- **DQN:** DQN can only handle discrete action spaces, so we discretized the action space and used the same environment as MAPPO.
- **Semantic-unaware:** This benchmark transmits all data without semantic extraction during offloading, i.e. $\mu_n = 1$. All other settings are identical to those used in MAPPO.
- **Local:** All tasks are executed locally.

B. QoE Performance and Convergence

1) *Convergence Performance:* The preference parameters, ω_t , ω_e , and ω_a are all set to 1/3, indicating that the model has no specific preference among latency, energy consumption, and accuracy. Fig. 6 shows that the MAPPO algorithm converges after approximately 50 episodes and maintains optimal performance. For the DQN algorithm, the replay buffer is set to 50 episodes, which causes a jump at 50 episodes in Fig. 7. The model finally converges after 350 episodes.

2) *QoE Performance:* Table. III presents the QoE performance without preference. All methods were given the same task queue and channel conditions as the exhaustive search

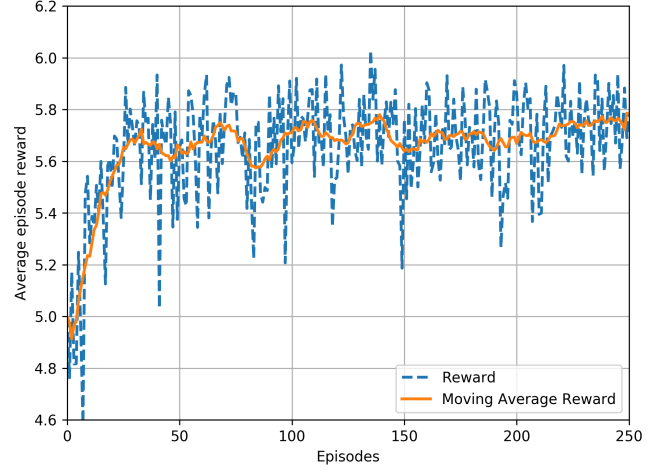


Fig. 6. Convergence of the MAPPO reward.

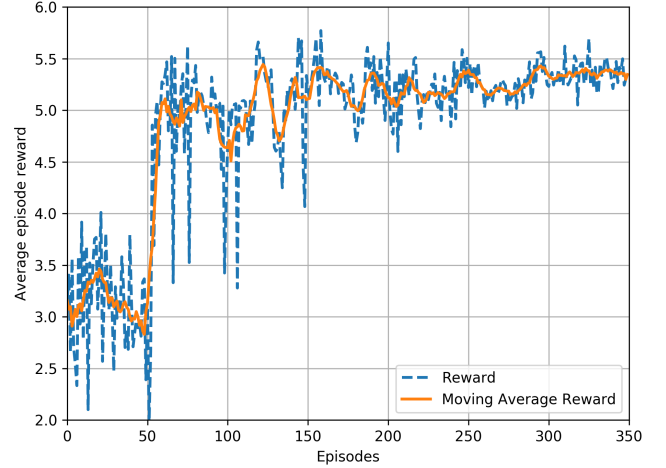


Fig. 7. Convergence of the DQN Reward.

to ensure fairness in comparisons. Table. III shows that the MAPPO method closely approaches the exhaustive search, demonstrating that our model performs near the optimal level. The semantic-unaware MAPPO method fixes $\mu_n = 1$ to transmit all data without any compression, resulting in increased transmission latency and reduced QoE compared to the MAPPO method. Conventional reinforcement learning approaches like DQN perform only slightly better than local execution. This is because DQN operates within a discrete action space and solely optimizes the value function. The proposed MAPPO method optimizes both the policy function and the value function, supporting a continuous action space, and thereby achieving near-optimal QoE. Local execution is solely related to the local computation frequency. When calculating QoE, the local computation frequency is fixed, meaning we use the local execution's latency, energy consumption, and accuracy to normalize the latency, energy, and accuracy obtained from other methods. Thus, the QoE of local execution is fixed at 0.5.

To further investigate the contributions of latency, energy

TABLE III
QoE PERFORMANCE WITHOUT PREFERENCE.

	Local	DQN	MAPPO	Semantic-Unaware MAPPO	Exhaustive Search
QoE	0.5	0.546	0.6	0.581	0.604

TABLE IV
ENERGY CONSUMPTION AND TASK PERFORMANCE WITHOUT PREFERENCE

	Local	DQN	MAPPO	Semantic-Unaware MAPPO
Energy Consumption (J)	1.37	3.05	3.19	3.60
Accuracy (%)	58.27	61.05	64.37	69.15

consumption, and task performance to QoE, Fig. 8 illustrates the execution latency when the task queue consists of mixed tasks. To eliminate the influence of task type distribution on execution latency, we tested 100 rounds and averaged the execution latency. Fig 8 shows that the MAPPO method has a lower task execution latency compared to the benchmarks. Although the DQN algorithm's overall QoE is lower than that of the semantic-unaware MAPPO method, its performance in execution latency is superior. This indicates that DQN's optimization focuses more on reducing execution latency. Then we fix the task queue for all UEs to consist of either text classification, image classification, or VQA, and test across 100 rounds to calculate the average. Fig. 9 further reveals the execution latency for different tasks. Text classification involves less computation than image classification and VQA, resulting in lower execution latency. It is evident that MAPPO achieves the lowest execution latency for all tasks. Local execution is the slowest across all task types. DQN and the semantic-unaware MAPPO method show very similar execution latencies for text classification tasks, while each has its strengths and weaknesses in image classification and VQA tasks.

In addition to execution latency, QoE also includes energy consumption and task performance. Table IV provides the energy consumption and task accuracy for all different schemes. Local execution has the lowest energy consumption, but its task accuracy is also the lowest. This is because local GPUs have limited computing power, and despite the lower energy consumption advantage compared to ES, it doesn't excel in task performance. The semantic-unaware method achieves the best task performance because it transmits significantly more data than the MAPPO method. However, this also results in higher energy consumption compared to the MAPPO method.

3) *QoE Preference*: We can adjust the model to achieve desired results by modifying QoE preferences for different metrics. Fig. 10 shows the performance of latency and task accuracy under different weights by adjusting the weights assigned to latency and accuracy. As the weight for latency increases, tasks are offloaded to the ES with more powerful processing capabilities, and there tends to be a preference for a smaller semantic extraction factor, μ_n , to maximize the compression rate. This results in a decrease in the accuracy of tasks executed by the ES. Fig. 11 presents the performance of energy consumption and task accuracy under different weights. A significant jump occurs at (0.67, 0.33) when the weight for accuracy increases, as tasks are offloaded to the ES, causing a

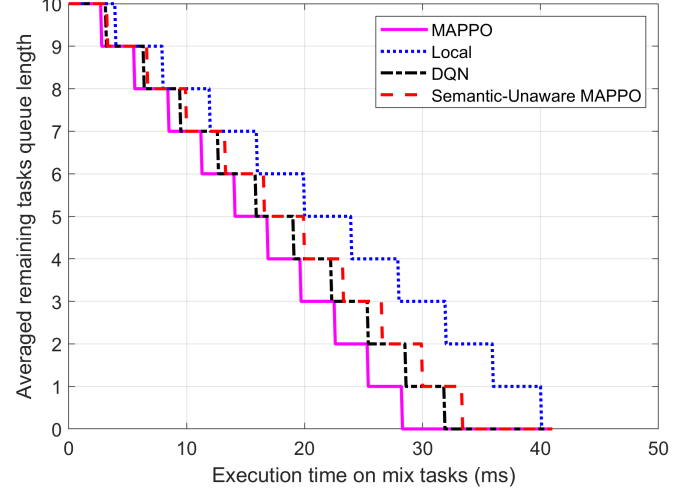


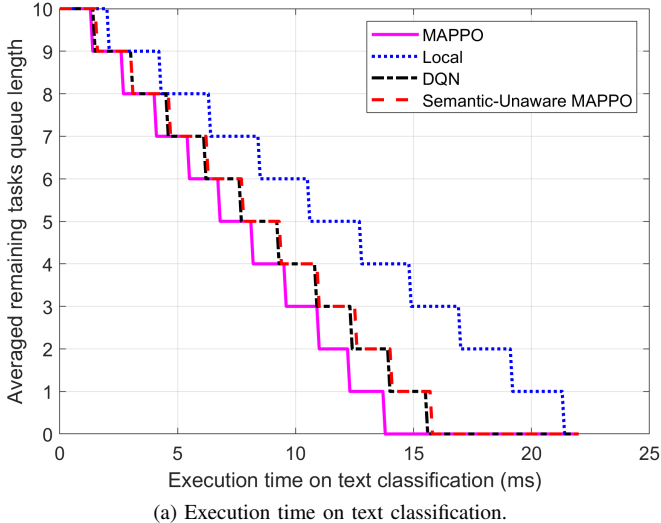
Fig. 8. Delay performance of mix tasks.

TABLE V
PERFORMANCE UNDER DIFFERENT PREFERENCES

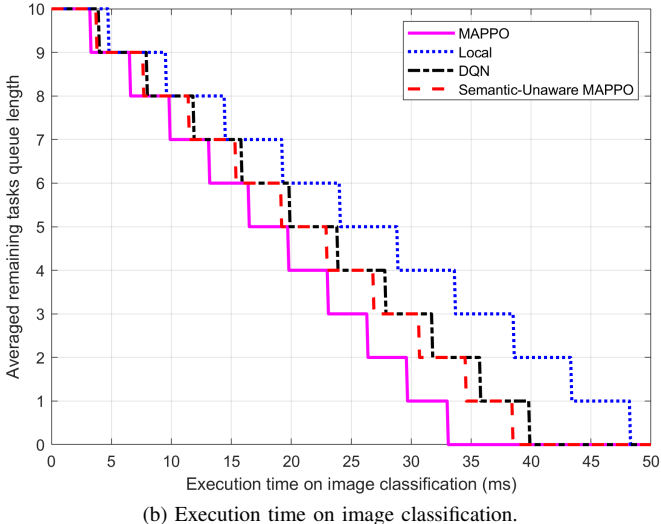
	Delay (ms)	Energy Consumption (J)	Accuracy (%)
No Preference	2.82	3.19	64.37
Delay Preference	2.18	2.66	54.08
Energy Preference	4.95	0.83	55.66
Accuracy Preference	3.25	3.49	68.57

substantial increase in energy consumption and a corresponding rise in accuracy. Fig. 12 describes the performance of energy consumption and latency under varying weights. When the weight for latency increases beyond (0.3, 0.7), latency begins to decrease, and energy consumption increases. This is due to an increase in the number of tasks offloaded to the ES, and users tend to choose a smaller semantic extraction factor, μ_n , to reduce data transmission volume. However, a smaller μ_n means that users need more computational resources to extract more compact semantic information.

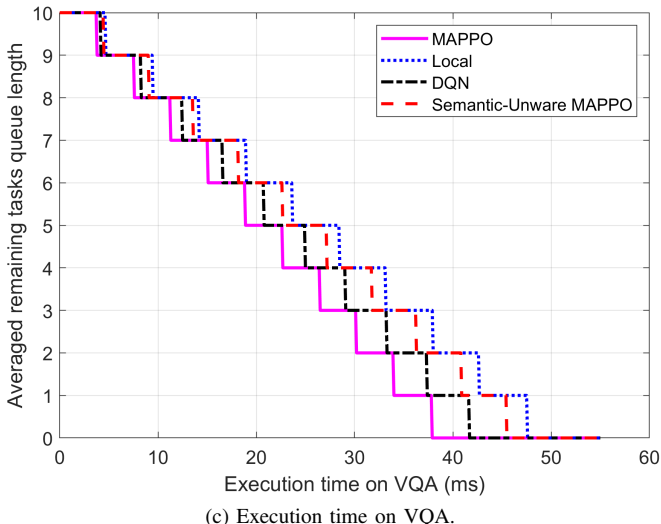
Table V shows the performance in execution latency, energy consumption, and task accuracy under varying preference settings. Specifically, we adjust the relative magnitude of ω_t , ω_e , and ω_a to set preferences for different metrics and retrain to obtain the corresponding model for each. 1) For the delay-preference model, we set $\omega_t = 1$, $\omega_e = 0$ and $\omega_a = 0$. The delay-preference model tends to choose a smaller μ_n to reduce the amount of data transmitted. This results in a partial loss of semantic information, causing a decline in task



(a) Execution time on text classification.



(b) Execution time on image classification.



(c) Execution time on VQA.

Fig. 9. Delay performance of different task modalities. Figs. (a), (b), and (c) depict the user task queue set for text classification, image classification, or VQA, respectively, and measure the task execution time for different methods.

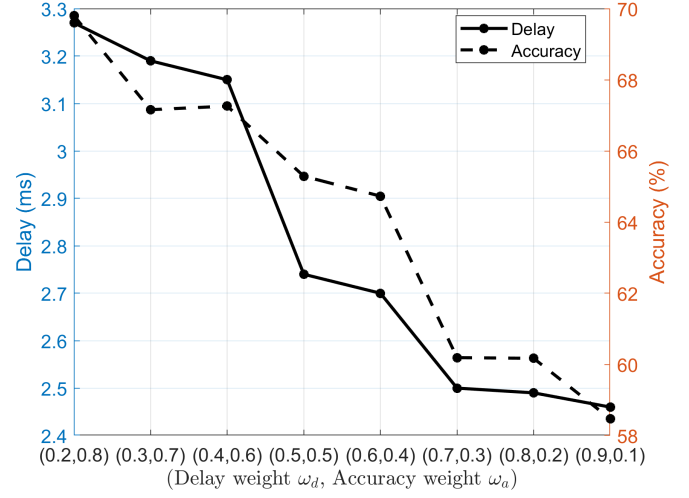


Fig. 10. Delay and accuracy performance with different weights.

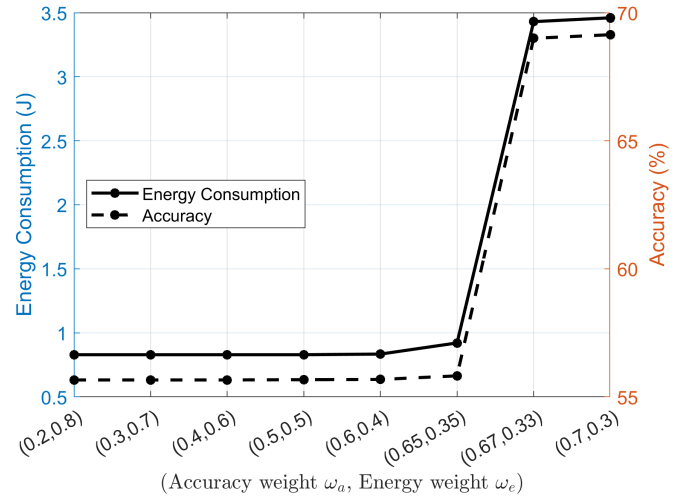


Fig. 11. Energy consumption and accuracy performance with different weights.

accuracy. 2) For the energy-preference model, we set $\omega_t = 0$, $\omega_e = 1$ and $\omega_a = 0$. The energy-preference model favors local execution, leading to significantly higher execution latency while reducing energy consumption. However, task accuracy is unsatisfactory. 3) For the accuracy-preference model, we set $\omega_t = 0$, $\omega_e = 0$ and $\omega_a = 1$. The accuracy-preference model aims to maximize the accuracy of all tasks, prompting it to choose a larger μ_n to preserve semantic information better. Nevertheless, transmitting a high volume of data results in higher overall energy consumption.

V. CONCLUSION

In this paper, we proposed a new multi-modal task offloading system and designed a unified quality of experience (QoE) metric to measure overall task offloading performance. Text classification, image classification, and visual question answering (VQA) tasks can be executed locally or offloaded to the edge server after semantic extraction. A multi-agent PPO reinforcement learning algorithm is used to solve the problem

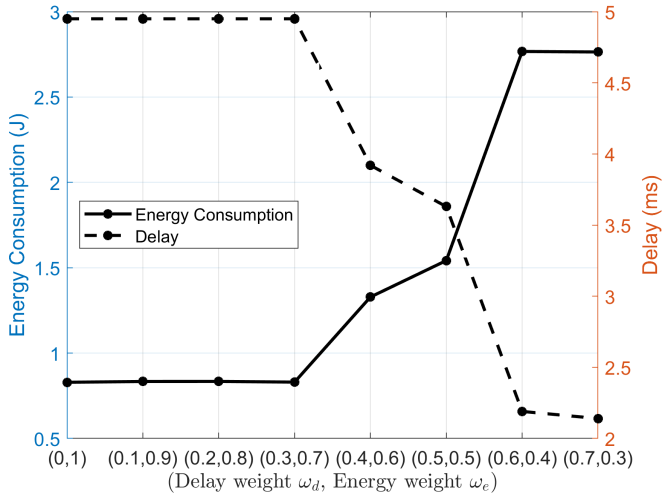


Fig. 12. Energy consumption and delay performance with different weights.

of maximizing overall user QoE through the joint optimization of the semantic extraction factor, computing resources, and communication resources. Experimental results show that the proposed method outperforms other benchmarks in overall user QoE. Specifically, the proposed algorithm achieves a reduction in execution latency and energy consumption of 18.1% and 12.9%, respectively compared to the semantic-unaware method. Additionally, the proposed approach can be flexibly adapted to user preferences, fully satisfying latency, energy, and task performance preference requirements.

REFERENCES

- I. A. Elgendi, W.-Z. Zhang, C.-Y. Liu, and C.-H. Hsu, "An Efficient and Secured Framework for Mobile Cloud Computing," *IEEE Transactions on Cloud Computing*, vol. 9, no. 1, pp. 79–87, 2021.
- S. Zhu, C. Liu, and Z. Xu, "High-Definition Video Compression System Based on Perception Guidance of Salient Information of a Convolutional Neural Network and HEVC Compression Domain," *IEEE Transactions on Circuits and Systems for Video Technology*, vol. 30, no. 7, pp. 1946–1959, 2020.
- L. Xia, Y. Sun, C. Liang, D. Feng, R. Cheng, Y. Yang, and M. A. Imran, "WiserVR: Semantic Communication Enabled Wireless Virtual Reality Delivery," *IEEE Wireless Communications*, vol. 30, no. 2, pp. 32–39, 2023.
- M. M. Rathore, A. Paul, W.-H. Hong, H. Seo, I. Awan, and S. Saeed, "Exploiting IoT and Big Data Analytics: Defining Smart Digital City Using Real-Time Urban Data," *Sustainable Cities and Society*, vol. 40, pp. 600–610, 2018.
- W. Weaver, "Recent Contributions to The Mathematical Theory of Communication," *ETC: A Review of General Semantics*, vol. 10, no. 4, pp. 261–281, 1953.
- H. Xie and Z. Qin, "A Lite Distributed Semantic Communication System for Internet of Things," *IEEE Journal on Selected Areas in Communications*, vol. 39, no. 1, pp. 142–153, 2021.
- H. Q. Xie, Z. J. Qin, G. Y. Li, and B. H. Juang, "Deep Learning Enabled Semantic Communication Systems," *IEEE Transactions on Signal Processing*, vol. 69, pp. 2663–2675, 2021.
- Y. N. Wang, M. Z. Chen, T. Luo, W. Saad, D. Niyato, H. V. Poor, and S. G. Cui, "Performance Optimization for Semantic Communications: An Attention-Based Reinforcement Learning Approach," *IEEE Journal on Selected Areas in Communications*, vol. 40, no. 9, pp. 2598–2613, 2022.
- E. Bourtsoulatze, D. B. Kurka, and D. Gündüz, "Deep Joint Source-Channel Coding for Wireless Image Transmission," *IEEE Transactions on Cognitive Communications and Networking*, vol. 5, no. 3, pp. 567–579, 2019.
- D. Huang, F. Gao, X. Tao, Q. Du, and J. Lu, "Toward Semantic Communications: Deep Learning-Based Image Semantic Coding," *IEEE Journal on Selected Areas in Communications*, vol. 41, no. 1, pp. 55–71, 2023.
- H. Zhang, H. Wang, Y. Li, K. Long, and A. Nallanathan, "DRL-Driven Dynamic Resource Allocation for Task-Oriented Semantic Communication," *IEEE Transactions on Communications*, vol. 71, no. 7, pp. 3992–4004, 2023.
- L. Galteri, M. Bertini, L. Seidenari, T. Uricchio, and A. Del Bimbo, "Increasing Video Perceptual Quality with GANs and Semantic Coding," in *Proceedings of the 28th ACM International Conference on Multimedia*. Seattle, WA, USA: Association for Computing Machinery, 2020, p. 862–870.
- P. Jiang, C. K. Wen, S. Jin, and G. Y. Li, "Wireless Semantic Communications for Video Conferencing," *IEEE Journal on Selected Areas in Communications*, vol. 41, no. 1, pp. 230–244, 2023.
- S. Wang, J. Dai, Z. Liang, K. Niu, Z. Si, C. Dong, X. Qin, and P. Zhang, "Wireless Deep Video Semantic Transmission," *IEEE Journal on Selected Areas in Communications*, vol. 41, no. 1, pp. 214–229, 2023.
- Y. Lin, H. Du, D. Niyato, J. Nie, J. Zhang, Y. Cheng, and Z. Yang, "Blockchain-Aided Secure Semantic Communication for AI-Generated Content in Metaverse," *IEEE Open Journal of the Computer Society*, vol. 4, pp. 72–83, 2023.
- L. Xia, Y. Sun, C. Liang, D. Feng, R. Cheng, Y. Yang, and M. A. Imran, "WiserVR: Semantic Communication Enabled Wireless Virtual Reality Delivery," *IEEE Wireless Communications*, vol. 30, no. 2, pp. 32–39, 2023.
- H. Du, J. Wang, D. Niyato, J. Kang, Z. Xiong, and D. I. Kim, "AI-Generated Incentive Mechanism and Full-Duplex Semantic Communications for Information Sharing," *IEEE Journal on Selected Areas in Communications*, vol. 41, no. 9, pp. 2981–2997, 2023.
- Z. Tian, H. Vo, C. Zhang, G. Min, and S. Yu, "An Asynchronous Multi-Task Semantic Communication Method," *IEEE Network*, 2023, early access, doi: 10.1109/MNET.2023.3321547.
- G. Zhang, Q. Hu, Z. Qin, Y. Cai, G. Yu, and X. Tao, "A Unified Multi-Task Semantic Communication System for Multimodal Data," *IEEE Transactions on Communications*, 2024, early access, doi: 10.1109/TCOMM.2024.3364990.
- H. Xie, Z. Qin, X. Tao, and K. B. Letaief, "Task-Oriented Multi-User Semantic Communications," *IEEE Journal on Selected Areas in Communications*, vol. 40, no. 9, pp. 2584–2597, 2022.
- A. C. Baktir, A. Ozgovde, and C. Ersoy, "How Can Edge Computing Benefit From Software-Defined Networking: A Survey, Use Cases, and Future Directions," *IEEE Communications Surveys & Tutorials*, vol. 19, no. 4, pp. 2359–2391, 2017.
- X. Deng, J. Li, L. Shi, Z. Wei, X. Zhou, and J. Yuan, "Wireless Powered Mobile Edge Computing: Dynamic Resource Allocation and Throughput Maximization," *IEEE Transactions on Mobile Computing*, vol. 21, no. 6, pp. 2271–2288, 2022.
- Y. Mao, J. Zhang, S. H. Song, and K. B. Letaief, "Power-Delay Tradeoff in Multi-User Mobile-Edge Computing Systems," in *2016 IEEE Global Communications Conference (GLOBECOM)*, Washington DC, USA, Conference Proceedings, pp. 1–6.
- C. F. Liu, M. Bennis, M. Debbah, and H. V. Poor, "Dynamic Task Offloading and Resource Allocation for Ultra-Reliable Low-Latency Edge Computing," *IEEE Transactions on Communications*, vol. 67, no. 6, pp. 4132–4150, 2019.
- S. Bi, L. Huang, H. Wang, and Y. J. A. Zhang, "Lyapunov-Guided Deep Reinforcement Learning for Stable Online Computation Offloading in Mobile-Edge Computing Networks," *IEEE Transactions on Wireless Communications*, vol. 20, no. 11, pp. 7519–7537, 2021.
- M. Min, L. Xiao, Y. Chen, P. Cheng, D. Wu, and W. Zhuang, "Learning-Based Computation Offloading for IoT Devices With Energy Harvesting," *IEEE Transactions on Vehicular Technology*, vol. 68, no. 2, pp. 1930–1941, 2019.
- H. Zhou, K. Jiang, X. Liu, X. Li, and V. C. M. Leung, "Deep Reinforcement Learning for Energy-Efficient Computation Offloading in Mobile-Edge Computing," *IEEE Internet of Things Journal*, vol. 9, no. 2, pp. 1517–1530, 2022.
- A. Clemm, M. T. Vega, H. K. Ravuri, T. Wauters, and F. D. Turck, "Toward Truly Immersive Holographic-Type Communication: Challenges and Solutions," *IEEE Communications Magazine*, vol. 58, no. 1, pp. 93–99, 2020.
- Y. Zhao, Z. Yang, X. He, X. Cai, X. Miao, and Q. Ma, "Trine: Cloud-Edge-Device Cooperated Real-Time Video Analysis for Household Applications," *IEEE Transactions on Mobile Computing*, vol. 22, no. 8, pp. 4973–4985, 2023.

- [30] Z. Qin, J. Ying, D. Yang, H. Wang, and X. Tao, "Computing Networks Enabled Semantic Communications," *IEEE Network*, pp. 1–1, 2024.
- [31] L. Yan, Z. Qin, R. Zhang, Y. Li, X. Tao, and G. Y. Li, "QoE-based Semantic-Aware Resource Allocation for Multi-Task Networks," *arXiv preprint arXiv:2305.06543*, 2023.
- [32] Y. Cang, M. Chen, Z. Yang, Y. Hu, Y. Wang, C. Huang, and Z. Zhang, "Online Resource Allocation for Semantic-Aware Edge Computing Systems," *IEEE Internet of Things Journal*, 2023, early access, doi: 10.1109/JIOT.2023.3325320.
- [33] Z. Ji and Z. Qin, "Computational Offloading in Semantic-Aware Cloud-Edge-End Collaborative Networks," *arXiv preprint arXiv:2402.18183*, 2024.
- [34] Z. Ji, Z. Qin, X. Tao, and Z. Han, "Resource Optimization for Semantic-Aware Networks with Task Offloading," *IEEE Transactions on Wireless Communications*, 2024, early access, doi: 10.1109/TWC.2024.3390407.
- [35] X. Hu, K.-K. Wong, and K. Yang, "Wireless Powered Cooperation-Assisted Mobile Edge Computing," *IEEE Transactions on Wireless Communications*, vol. 17, no. 4, pp. 2375–2388, 2018.
- [36] X. Ma, A. Zhou, S. Zhang, and S. Wang, "Cooperative Service Caching and Workload Scheduling in Mobile Edge Computing," in *IEEE INFO-COM 2020 - IEEE Conference on Computer Communications*, 2020, pp. 2076–2085.
- [37] Z. Jin, C. Zhang, Y. Jin, L. Zhang, and J. Su, "A Resource Allocation Scheme for Joint Optimizing Energy Consumption and Delay in Collaborative Edge Computing-Based Industrial IoT," *IEEE Transactions on Industrial Informatics*, vol. 18, no. 9, pp. 6236–6243, 2022.
- [38] N. Cheng, F. Chen, W. Chen, Z. Cheng, Q. Yang, C. Li, and X. Shen, "6G Omni-Scenario On-Demand Services Provisioning: Vision, Technology and Prospect," *SCIENCE CHINA Information Sciences*, vol. 54, no. 5, pp. 1025–1054, 2024.
- [39] S.-W. Ko, K. Han, and K. Huang, "Wireless Networks for Mobile Edge Computing: Spatial Modeling and Latency Analysis," *IEEE Transactions on Wireless Communications*, vol. 17, no. 8, pp. 5225–5240, 2018.
- [40] P. Mach and Z. Becvar, "Mobile Edge Computing: A Survey on Architecture and Computation Offloading," *IEEE Communications Surveys & Tutorials*, vol. 19, no. 3, pp. 1628–1656, 2017.
- [41] S. Li, J. Huang, J. Hu, and B. Cheng, "QoE-DEER: A QoE-Aware Decentralized Resource Allocation Scheme for Edge Computing," *IEEE Transactions on Cognitive Communications and Networking*, vol. 8, no. 2, pp. 1059–1073, 2022.
- [42] M. Hemmati, B. McCormick, and S. Shirmohammadi, "QoE-Aware Bandwidth Allocation for Video Traffic Using Sigmoidal Programming," *IEEE MultiMedia*, vol. 24, no. 4, pp. 80–90, 2017.
- [43] L. Yan, Z. Qin, C. Li, R. Zhang, Y. Li, and X. Tao, "QoE-based Semantic-Aware Resource Allocation for Multi-Task Networks," *IEEE Transactions on Wireless Communications*, pp. 1–1, 2024.
- [44] J. Schulman, P. Moritz, S. Levine, M. Jordan, and P. Abbeel, "High-Dimensional Continuous Control Using Generalized Advantage Estimation," *arXiv preprint arXiv:1506.02438*, 2015.
- [45] J. Devlin, M.-W. Chang, K. Lee, and K. Toutanova, "BERT: Pre-training of Deep Bidirectional Transformers for Language Understanding," *arXiv preprint arXiv:1810.04805*, 2018.
- [46] A. Dosovitskiy, L. Beyer, A. Kolesnikov, D. Weissenborn, X. Zhai, T. Unterthiner, M. Dehghani, M. Minderer, G. Heigold, S. Gelly, J. Uszkoreit, and N. Houlsby, "An Image is Worth 16x16 Words: Transformers for Image Recognition at Scale," in *International Conference on Learning Representations*, 2021.